Near-infrared photon time-of-flight spectroscopy of turbid materials up to 1400 nm

Tomas Svensson,[1] Erik Alerstam,[1] Dmitry Khoptyar,[1] Jonas Johansson,[2] Staffan Folestad,[2] and Stefan Andersson-Engels[1]
[1]*Department of Physics, Lund University, P.O. Box 118, S-221 00 Lund, Sweden*
[2]*Astra Zeneca R&D, 431 83 Mölndal, Sweden*

(Received 23 March 2009; accepted 29 May 2009; published online 23 June 2009)

Photon time-of-flight spectroscopy (PTOFS) is a powerful tool for analysis of turbid materials. We have constructed a time-of-flight spectrometer based on a supercontinuum fiber laser, acousto-optical tunable filtering, and an InP/InGaAsP microchannel plate photomultiplier tube. The system is capable of performing PTOFS up to 1400 nm, and thus covers an important region for vibrational spectroscopy of solid samples. The development significantly increases the applicability of PTOFS for analysis of chemical content and physical properties of turbid media. The great value of the proposed approach is illustrated by revealing the distinct absorption features of turbid epoxy resin. Promising future applications of the approach are discussed, including quantitative assessment of pharmaceuticals, powder analysis, and calibration-free near-infrared spectroscopy. © *2009 American Institute of Physics.* [DOI: 10.1063/1.3156047]

Near infrared (NIR) radiation was discovered in a famous experiment by Herschel in 1800. By using a prism and a thermometer, Herschel discovered that the heat in sunlight not only comes from visible radiation. Although the exploration of the analytical importance of this discovery was not initiated earlier than almost 150 years later, near-infrared spectroscopy (NIRS) is today a well established technique for analytical chemistry and of great importance for numerous fields of science and technology.[1,2]

NIR spectral features are typically due to relatively weak overtones and combination bands of the fundamental vibrational transitions found in the mid-infrared. This origin explains why many materials exhibit fairly low absorption in the NIR spectral region (750–2500 nm). This gives NIRS the rather unique ability of performing nondestructive and noninvasive analysis of solid and liquid samples without a need for sample preparation. This advantage of deep light penetration has made NIRS a very important tool in analysis of important materials such as foods and agricultural products,[3] biological tissue,[4–7] and pharmaceutical solids.[8,9] A general complication in this context is that microscopic variations in the refractive index renders these materials highly light scattering (turbid). As a result, optical path lengths are unknown, and detected intensity levels vary strongly with physical properties of the sample (i.e., intensity varies not only with chemical properties, one measures absorbance rather than absorption). Although this makes NIRS capable of not only chemical analysis but also analysis and prediction of physical properties of materials such as particle size, coating thickness, and hardness, these facts (in combination with the rather nonselective character of broad and overlapping NIR spectral features) have made conventional (steady-state) NIRS reliant on sophisticated calibration schemes in which all possible/relevant variations in physical and chemical properties should be covered.[8] This is, however, difficult to achieve in practice, and is more or less impossible in the important case of biological and clinical applications of NIRS.

Although it requires the use of significantly more sophisticated technology than conventional NIRS, the complications discussed above can be circumvented, and the effects of structural parameters (light scattering) and chemical composition (light absorption) can be distinguished. By employing pulsed illumination and time-resolved detection of diffuse reflectance or transmittance (with picosecond time resolution), photon time-of-flight (TOF) distributions can be measured. When involving multiple wavelengths, the technique is referred to as photon time-of-flight spectroscopy (PTOFS). A simple approach in deriving absorption coefficients from TOF distributions is then to utilize the recorded intensity decay in combination with the Beer–Lambert–Bouguer theory of absorption [$I=I_0 \exp(-\mu_a ct)$, where μ_a is the absorption coefficient and c is the speed of light].[5] More accurate results can be obtained by proper modeling of light propagation in turbid media, e.g., by means of diffusion theory[10] or a scheme for inverse Monte Carlo.[11,12] In addition, such refined data evaluation enables quantitative determination of both absorption coefficients, μ_a, and reduced scattering coefficients, μ_s' (i.e., provide deconvoluted information about both chemical composition and structural properties). It should be noted that the time-domain method (pulsed illumination), of course, has its correspondent in the frequency domain, often referred to as frequency domain photon migration (phase and amplitude recordings at multiple modulation frequencies[13]). Prominent examples of these two related techniques include *in vivo* blood monitoring,[5,14,15] breast cancer diagnostics via detection of intrinsic tumor biomarkers,[7] studies of brain hemodynamics and cerebral oxygenation,[16,17] and diffuse optical tomography.[18] Emerging applications include calibration-free and quantitative analysis of pharmaceutical solids,[19] scatter correction of NIRS of pharmaceutical solids,[20] particle size

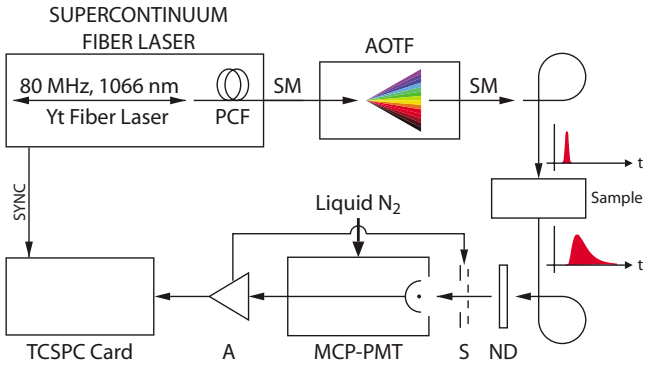

FIG. 1. (Color online) Setup schematic. The SC fiber laser is based on an ytterbium fiber laser that generates pulsed white light by means of nonlinear effects in a photonic crystal fiber (PCF). Adjustable AOTFs (single mode, SM, fiber coupled) are used to obtain narrow bandwidth pulses centered around any wavelength within their operational range. Light pulses injected in the turbid samples broaden due to multiple scattering, and the resulting TOF distribution is measured with a MCP-PMT in combination with TCSPC. The detector used for the 1100–1400 nm range requires liquid nitrogen cooling. A shutter (s) protects the MCP-PMT from excess optical power via feedback from the amplifier (a), and the detected intensity is controlled via a neutral density (ND) filter wheel.

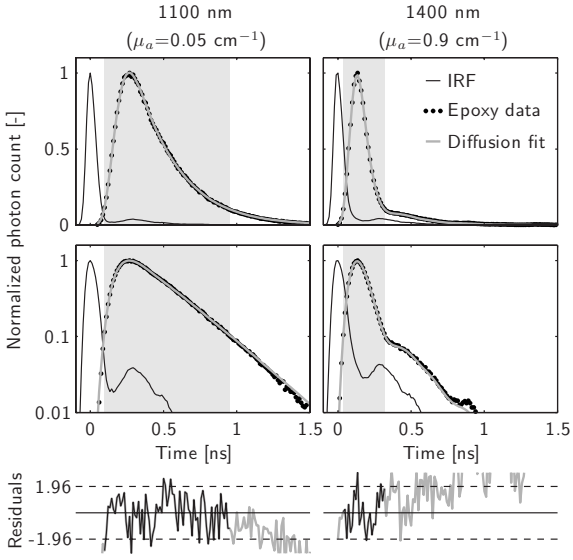

FIG. 2. NIR PTOFS data (linear and logarithmic scale) from a 3 mm thick phantom designed to mimic the extreme levels of scattering in pharmaceutical tablets. The figure also shows typical diffusion model fits and corresponding residuals. Fitting is performed over the top order of magnitude (this range is marked by gray shading, and corresponding residuals are plotted black). The residuals are weighted by the square root of the photon count and are expected to be distributed according to a standardized normal distribution (the [−1.96,1.96] range marks its 95% confidence interval). High absorption results in a very narrow TOF distribution at 1400 nm (μ_a =0.9 cm^{-1}, right column), while the absorption is significantly lower at 1100 nm (μ_a=0.05 cm^{-1}, left column). Both IRFs are approximately 75 ps FWHM.

analysis,[21] as well as optical porosimetry (PTOFS in combination with gas sensing).[22]

Until now, PTOFS has been limited to the spectral range below 1100 nm (i.e., above ~9100 cm^{-1}).[23–25] As most diagnostically important spectral features for vibrational spectroscopy are found at longer wavelengths, this is indeed a severe limitation of the technique. In this paper we extend the operational range of PTOFS up to 1400 nm, thus dramatically increasing the applicability of PTOFS for analytical chemistry of turbid materials.

Our novel experimental setup is illustrated in Fig. 1. A state-of-the-art supercontinuum (SC) fiber laser (Fianum SC-500–6, 80 MHz repetition rate) supplies pulsed illumination over the wide range of 500–1850 nm, and the use of two acousto-optical tunable filters (AOTFs) (Crystal Technology) allows wavelength selective excitation (each having different operation ranges: 650–1100 and 900–1550 nm, respectively). In the 650–1400 nm range, obtained pulses are typically shorter than 50 ps full width at half maximum (FWHM) and covering less than 8 nm FWHM. Light is delivered to the sample via a 600 μm diameter graded-index optical fiber (G600/840N, A.R.T. Photonics). After passing through the turbid sample, transmitted diffuse light is collected by a second fiber and delivered to a fast microchannel plate photomultiplier tube (MCP-PMT). The MCP-PMT output is controlled and amplified (HFAC-26, Becker&Hickl) and photon TOF distributions are measured by means of time-correlated single photon counting (TCSPC) (SPC-300, Becker&Hickl). In order to reach as far as up to 1400 nm, we employ an InP/InGaAsP MCP-PMT (NIR-PMT) that covers at the 1000–1400 nm spectral range (R3809U-68, Hamamatsu Photonics). A second MCP-PMT (R3809-59, Hamamatsu Photonics) allows measurements in the visible range and below 1000 nm (vis-PMT). In evaluation of PTOFS data, it is essential to take the instrumental response function (IRF) into account. The IRF is recorded by replacing the sample with a thin sheet of paper coated with toner. Experimental data are evaluated by being compared to a convolution between the IRF and theoretical impulse responses in a Levenberg–Marquardt (iterative) curve fitting procedure[12] (resulting in estimations of absorption and scattering coefficients). In this work, we analyze the data by fitting a diffusion model of light propagation in turbid slabs,[26] assuming a refractive index of 1.55.[27]

We demonstrate the capability of this system by investigating the NIR optical properties of a TiO_2-based epoxy phantom. Such phantoms are commonly used within the field of biomedical optics, and the particular sample examined here was used in Ref. 22 (cylindrical shape, 10 mm in diameter and 3 mm thick).

Raw PTOFS data from the NIR region are shown in Fig. 2 and give examples of measurements at both low and high absorption. In this work, fitting is constrained to one order of magnitude (the region with highest photon count). Utilizing a larger part of the dynamic range can further improve performance, but requires further studies of accuracy and dynamic range in IRF recordings.

An overview of the optical properties in the visible and NIR range is given in Fig. 3, and provides a striking example of the value added by extending spectral coverage above 1100 nm. The smooth decay of scattering with wavelength ensures instrumental stability, and the rate of this decay agrees with earlier experience TiO_2-based phantoms. Moreover, the structure of the absorption spectra below 1100 nm is in good agreement with earlier findings for similar phantom materials.[28] It should be noted that spectral distortions due to the wide spectral bandpass has been shown to be an important effect in PTOFS,[29] but is not discussed further here.

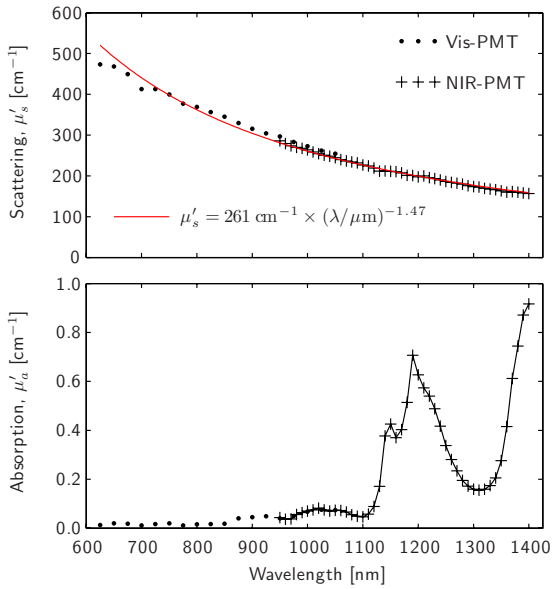

FIG. 3. (Color online) Summary of derived optical properties (as derived from diffusion theory). Measurements with the NIR-PMT were repeated twice, and the average day-to-day reproducibilities were 0.7% for μ_s' and 3% for μ_a. As expected from the general Mie theory, scattering decays smoothly with wavelength. A fitted $a \times (\lambda/\mu\mathrm{m})^b$ Mie-type curve is shown for reference. The derived absorption spectra exhibit distinct and heavily modulated features above 1100 nm, mainly due to the second overtone CH bands (around 1200 nm) and first overtone OH bands (around 1400 nm).

In summary, the progress reported here shows that PTOFS can now reach the diagnostically important overtone and combinational bands found in the 1100–1400 nm spectral range. While earlier applications of PTOFS are mainly restricted to medical spectroscopy, this development opens for numerous completely new applications within analytical chemistry of turbid materials. In particular, the extended spectral coverage makes PTOFS especially suited for NIRS of pharmaceutical solids (e.g., tablets and powders). With the inherent capability of separating scattering from absorption in combination with the ability to quantify absorption coefficients, PTOFS will greatly simplify calibration efforts in assessment of chemical content. This is a great advantage with respect to conventional NIRS of pharmaceutical solids, a technique which is very sensitive to variations in physical properties (scattering) and requires sophisticated calibration schemes.

[1] M. Blanco and I. Villarroya, TrAC Trends Anal. Chem. **21**, 240 (2002).
[2] H. W. Siesler, Y. Ozaki, S. Kawata, and H. M. Heise, *Near-Infrared Spectroscopy: Principles, Instruments, Applications* (Wiley, New York, 2002).
[3] H. Huang, H. Yu, H. Xu, and Y. Ying, J. Food Eng. **87**, 303 (2008).
[4] G. Millikan, Rev. Sci. Instrum. **13**, 434 (1942).
[5] B. Chance, J. Leigh, H. Miyake, D. Smith, S. Nioka, R. Greenfeld, M. Finander, K. Kaufmann, W. Levy, M. Young, P. Cohen, H. Yoshioka, and R. Boretsky, Proc. Natl. Acad. Sci. U.S.A. **85**, 4971 (1988).
[6] M. Wolf, M. Ferrari, and V. Quaresima, J. Biomed. Opt. **12**, 062104 (2007).
[7] S. Kukreti, A. Cerussi, B. Tromberg, and E. Gratton, J. Biomed. Opt. **12**, 020509 (2007).
[8] M. Blanco, J. Coello, H. Iturriaga, S. Maspoch, and C. de la Pezuela, Analyst (Cambridge, U.K.) **123**, 135R (1998).
[9] G. Reich, Adv. Drug Delivery Rev. **57**, 1109 (2005).
[10] M. Patterson, B. Chance, and B. Wilson, Appl. Opt. **28**, 2331 (1989).
[11] E. Alerstam, S. Andersson-Engels, and T. Svensson, J. Biomed. Opt. **13**, 041304 (2008).
[12] E. Alerstam, S. Andersson-Engels, and T. Svensson, Opt. Express **16**, 10440 (2008).
[13] B. Chance, M. Cope, E. Gratton, N. Ramanujam, and B. Tromberg, Rev. Sci. Instrum. **69**, 3457 (1998).
[14] B. Chance, S. Nioka, J. Kent, K. Mccully, M. Fountain, R. Greenfeld, and G. Holtom, Anal. Biochem. **174**, 698 (1988).
[15] T. Svensson, E. Alerstam, M. Einarsdóttír, K. Svanberg, and S. Andersson-Engels, J. Biophoton. **1**, 200 (2008).
[16] J. Hebden, A. Gibson, R. Yusof, N. Everdell, E. Hillman, D. Delpy, S. Arridge, T. Austin, J. Meek, and J. Wyatt, Phys. Med. Biol. **47**, 4155 (2002).
[17] E. Gratton, V. Toronov, U. Wolf, M. Wolf, and A. Webb, J. Biomed. Opt. **10**, 011008 (2005).
[18] J. Hebden and D. Delpy, Opt. Lett. **19**, 311 (1994).
[19] J. Johansson, S. Folestad, M. Josefson, A. Sparen, C. Abrahamsson, S. Andersson-Engels, and S. Svanberg, Appl. Spectrosc. **56**, 725 (2002).
[20] C. Abrahamsson, A. Löwgren, B. Strömdahl, T. Svensson, S. Andersson-Engels, J. Johansson, and S. Folestad, Appl. Spectrosc. **59**, 1381 (2005).
[21] F. Pandozzi and D. Burns, Anal. Chem. **79**, 6792 (2007).
[22] T. Svensson, M. Andersson, L. Rippe, S. Svanberg, S. Andersson-Engels, J. Johansson, and S. Folestad, Appl. Phys. B: Lasers Opt. **90**, 345 (2008).
[23] C. Abrahamsson, T. Svensson, S. Svanberg, S. Andersson-Engels, J. Johansson, and S. Folestad, Opt. Express **12**, 4103 (2004).
[24] A. Pifferi, A. Torricelli, P. Taroni, D. Comelli, A. Bassi, and R. Cubeddu, Rev. Sci. Instrum. **78**, 053103 (2007).
[25] A. Bassi, J. Swartling, C. D'Andrea, A. Pifferi, A. Torricelli, and R. Cubeddu, Opt. Lett. **29**, 2405 (2004).
[26] D. Contini, F. Martelli, and G. Zaccanti, Appl. Opt. **36**, 4587 (1997).
[27] M. Firbank and D. Delpy, Phys. Med. Biol. **38**, 847 (1993).
[28] A. Pifferi, A. Torricelli, A. Bassi, P. Taroni, R. Cubeddu, H. Wabnitz, D. Grosenick, M. Moller, R. MacDonald, J. Swartling, T. Svensson, S. Andersson-Engels, R. van Veen, H. Sterenborg, J. Tualle, H. Nghiem, S. Avrillier, M. Whelan, and H. Stamm, Appl. Opt. **44**, 2104 (2005).
[29] A. Farina, A. Bassi, A. Pifferi, P. Taroni, D. Comelli, L. Spinelli, and R. Cubeddu, Appl. Spectrosc. **63**, 48 (2009).